# Rethinking the design of a 2-methoxy-2-methyl-heptane process by unraveling the true thermodynamics and kinetics

Patrașcu, Iulian; Bîldea, Costin Sorin; Kiss, Anton A.

**DOI**
10.1016/j.cherd.2021.12.002

**Publication date**
2022

**Document Version**
Final published version

**Published in**
Chemical Engineering Research and Design

Contents lists available at ScienceDirect

Chemical Engineering Research and Design

journal homepage: www.elsevier.com/locate/cherd

# Rethinking the design of a 2-methoxy-2-methyl-heptane process by unraveling the true thermodynamics and kinetics

*Iulian Patraşcu*[a,*], *Costin Sorin Bîldea*[a], *Anton A. Kiss*[b,c]

[a] *University "Politehnica" of Bucharest, Polizu 1-7, 011061 Bucharest, Romania*
[b] *Department of Chemical Engineering and Analytical Science, The University of Manchester, Sackville Street, Manchester M13 9PL, United Kingdom*
[c] *Department of Chemical Engineering, Delft University of Technology, Van der Maasweg 9, 2629 HZ Delft, The Netherlands*

ARTICLE INFO

*Article history:*
Received 8 September 2021
Received in revised form 20 November 2021
Accepted 1 December 2021
Available online 6 December 2021

*Keywords:*
2-Methoxy-2-methyl-heptane
Process design
Plantwide control
Process simulation

ABSTRACT

Among other fuel additives — such as MTBE, ETBE, or TAME — 2-methoxy-2-methyl heptane (MMH) can increase the fuel octane number and reduce the CO emission. MMH can be obtained through the exothermal etherification of 2-methyl-1-heptene and methanol. Lately, many researchers have developed more and more efficient processes considering the kinetics corresponding to an endothermal reaction. However, in this work we demonstrate that the reaction is actually quite exothermal, and this has strong impact on the designed process. Also, the vapor–liquid equilibrium data predicted by UNIQUAC model for 2-methoxy-2-methyl heptane and 2-methyl-2-heptanol mixture reveals that product purification is more difficult, and it requires more energy to recover and obtain MMH with high purity. Considering these aspects, the 54.87 ktpy process developed in this paper is more realistic and energy intensive (1.82 kW h/kg MMH), with a TAC of 5.3 M$/year. The controllability of the process is proven for ±20% changes of 2-methoxy-2-methyl-heptane production rate.



## 1. Introduction

Octane numbers of ethers are high, and for this reason they have been used as octane boosters in gasoline. Among other tertiary ethers (such as MTBE, ETBE or TAME), 2-methoxy-2-methyl heptane (MMH) improves well the combustion of gasoline by reducing the CO emissions and enhancing the cold weather drivability (Karinen and Krause, 1999). Additionally, MMH has a high-molecular weight, which makes it less soluble in water. MMH can be produced by the reversible reaction between 2-methyl-1-heptene (MH) and methanol (MeOH), in the presence of solid acid catalysts such as Amberlyst 35 (Karinen and Krause, 1999). The etherification is accompanied by side reactions amongst which the most important are the isomerization of 2-methyl-1-heptene to 2-methyl-2-heptene, dehydration of methanol to di-methyl-ether (DME) and the addition of resulting water to alkenes resulting in 2-methyl-2-heptanol (MHOH). Several industrial-scale processes for production of MMH has been proposed. Griffin et al. (2009) present the flowsheet of a conventional (Reaction–Separation–Recycle) MMH production process and illustrate the effect of changing the equilibrium constant on the optimal operating point, without giving details regarding units sizing. The process is further considered by Luyben (2010) who use it to illustrate the trade-offs between reactor size and recycle. Detailed equipment sizing, economic evaluation and plantwide control are presented. The design of Luyben (2010) is further optimized by changing the operating pressures, number of stages and feed stage location of the three distillation columns in a recent paper (Hussain et al., 2021). Moreover, significant energy and capital savings are achieved by replacing two distillation columns by an intensified dividing wall configuration (Hussain et al., 2021). Hussain et al. (2018) describes process for MMH production based on reactive distillation and employing heat integration, which shows good economics. To deal with the large amount of catalyst which leads to a large diameter of the RD column, Hussain and Lee (2018) design a side-reactor column (SRC)

* *Corresponding author.*
E-mail address: patrascu.iulian90@yahoo.ro (I. Patraşcu).
https://doi.org/10.1016/j.cherd.2021.12.002

configuration. The effect of operating pressure on process intensification in the SRC process is further discussed by Hussain et al. (2019).

This literature review shows that there is much interest in design, economic evaluation and plantwide control of industrial MMH production processes. However, as it will be shown in the next section, the kinetics used in the previous papers is unrealistic. More precisely, the kinetics of the MMH formation reaction which was used in the previous studies corresponds to an endothermal reversible reaction. Considering both chemical equilibrium and reaction rate, endothermal reversible reactions are favored by high temperature. However, as many other etherification reactions between alkenes and alcohols, the reaction between MH and MeOH is slightly exothermal. In this case, high temperature leads to an increase of reaction rate, but the maximum achievable conversion decreases according to Le Chatelier's principle.

Previous studies used a perfectly mixed reactor model (CSTR). From the selectivity point of view, this is useful for the parallel–consecutive reaction stoichiometry of the MMH process. However, because large amounts of catalyst are used, mixing is quite difficult. In this case, a fixed bed catalytic reactor is realistic, but a high selectivity is more difficult to achieve.

The separation of MMH product from MHOH by product is an important part of the process. The difficulty of this step is given by the vapor–liquid equilibria. Due to the lack of the thermodynamic data, previous studies used predictive models for MHOH properties, amongst which the vapor pressure is of particular interest. These models predict large difference in the MMH and MHOH boiling points, thus the separation appears to be easy. In this work we show that a better vapor pressure model is available for MHOH. When this model is used, the MMH/MHOH separation appears to be more difficult than previously thought.

The goal and novelty of this paper is to re-examine the design, economics and plantwide control of the conventional Reaction–Separation–Recycle MMH process, considering a better model of the MHOH vapor pressure, the more realistic kinetics of the main reaction (exothermal etherification reaction of MH with methanol), and a reaction system involving a multi-bed catalytic reactor with interstage cooling that can be actually built in practice.

The article is organized as follows: the thermodynamic basis is discussed in the next section, with emphasis on the vapor–liquid equilibrium (VLE) in the MMH–MHOH the system. Then, the reaction thermodynamics is considered, reconciliating the chemical kinetics and heat effect, which now both corresponds to an exothermal reaction. The next section discusses the consequences of using a fixed bed catalytic reactor on the achievable selectivity. All these considerations are used to design a more realistic process. Economic evaluation shows that the costs of MMH production are much larger than previously thought. The last section considers plantwide control issues, demonstrating the controllability of the process. The paper ends with conclusions.

## 2. Vapor–liquid equilibrium

The UNIQUAC method is selected in Aspen Plus v10.0 to calculate the physical properties. MeOH, MH, DME and MHOH were found in the Aspen Plus database, while MMH was introduced as a user-defined component. The binary interaction parameters for the DME-MeOH pair are available in the Aspen Plus database, for the other pairs being estimated by the UNIFAC method. The normal boiling points (n.b.p) are −24.84 °C (DME), 64.7 °C (MeOH), 119.22 °C (MH), 151.36 °C (MMH), 158.94 (MHOH). Aspen predicts a heterogeneous MeOH-MH azeotrope (n.b.p. 62.5 °C), but this does not lead to any difficulty because MeOH and MH are reactants, adjacent in the order of volatility. Thus, their separation is not necessary, being recycled together. The separation of DME and of MMH + MHOH from the reactants seem easy. However, the MMH–MHOH split is more difficult, the difference in the boiling points being less than 8 °C. This contradicts the findings of the previous studies on MMH production, where all the separations were easy. To explain this difference, we remark that, in all previous studies, MHOH was a user defined component in Aspen Plus, for which the physical properties were estimated by various group contribution methods. When MHOH is introduced as a user-defined component, Aspen Plus Property Constant Estimation System (PCES) predicts that the n.b.p. of MHOH is 198.24 °C. Thus, the difference between MMH and MHOH boiling points is large, and the separation appears to be easy. A closer look at the source of different physical properties reveals that the n.b.p. of the user defined MHOH is PCES (Joback method) and the vapor pressure is calculated by the extended Antoine equation with PLXANT parameters estimated by the Riedel method. In contrast, the vapor pressure of the database MHOH is calculated by NIST Wagner 25 equation, with parameters retrieved from the NIST-TRC database. The PubChem database lists the MHOH experimental n.b.p as being 156.0 °C (pubchem.ncbi.nlm.nih.gov/compound/12242), while the U.S. Environmental Protection Agency (comptox.epa.gov/dashboard/chemical/properties/DTXSID00211538) gives 156 ± 1 °C as the experimental average. These values are very close to the n.b.p. of the database component, but very different from the value predicted for the user-defined component.

Fig. 1 (left) shows the MHOH vapor pressure, calculated with the Wagner 25 equation with NIST-TRC parameters (database component) and with the extended Antoine equation with estimated parameters (user defined component). Clearly, the user defined component appears to be much less volatile. Fig. 1 (right) presents in the Txy diagram the vapor–liquid equilibrium in the MMH–MHOH system, at 0.1 bar, calculated in two different ways. This shows that the MHOH-MMH separation by distillation is more difficult than previously thought, especially when high purity MMH is required. This has a negative impact on the investment and operating costs (more separation stages needed, larger energy requirements).

## 3. Chemical equilibrium

The main reaction in the 2-methyl-2-methoxy heptane process is the addition of methanol to 2-methyl-2-heptene, according to Reaction (1).

$$\underset{\text{(MeOH)}}{CH_3OH} + \underset{\text{(MH)}}{C_8H_{16}} \rightleftarrows \underset{\text{(MMH)}}{C_8H_{17}OCH_3} \quad (1)$$

Previous studies described the MMH formation rate by a mole-fraction based, power-law, reversible kinetics, Eq. (2):

$$r_1 = k_{1F} x_{MeOH} x_{MH} - k_{1R} x_{MMH} \quad (2)$$

where the rate constants of the forward and reverse reactions are:

$$k_{1F} / \left[\text{kmol} \times \text{s}^{-1} \times \text{kg}_{\text{cat}}^{-1}\right] = 6.7 \times 10^7 \cdot \exp\left(-\frac{90,000\,[\text{kJ/kmol}]}{RT}\right) \quad (3)$$

$$k_{1R} / \left[\text{kmol} \times \text{s}^{-1} \times \text{kg}_{\text{cat}}^{-1}\right] = 2.1 \times 10^{-6} \cdot \exp\left(-\frac{900\,[\text{kJ/kmol}]}{RT}\right) \quad (4)$$

Therefore, the corresponding equilibrium constant is:

$$K_{x,1} = \frac{k_{1F}}{k_{1R}} = 3.19 \times 10^{13} \cdot \exp\left(-\frac{89,100\,[\text{kJ/kmol}]}{RT}\right) \quad (5)$$

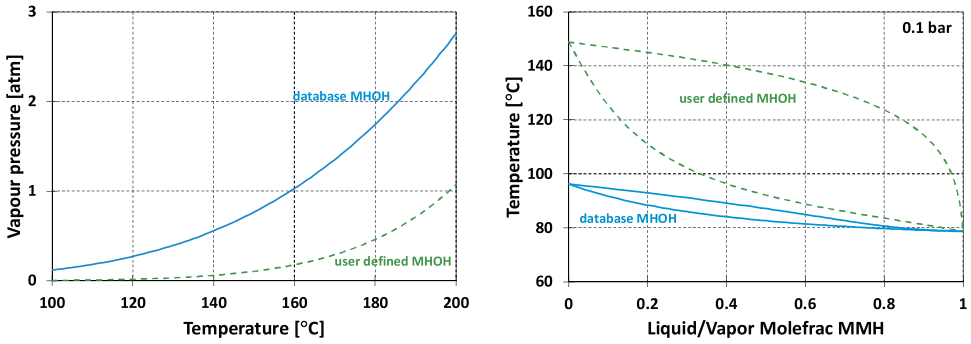


**Fig. 1 – Left: MHOH vapor pressure vs. temperature calculated by the Wagner 25 equation with NIST-TRC parameters (database MHOH, continuous line) and by the extended Antoine equation with parameters estimated by Riedel method (user defined MHOH, dashed line). Right: vapor liquid equilibrium in the MMH–MHOH system, with MHOH properties calculated in different ways.**

or, equivalently:

$$\ln K_{x,1} = 31.09 - \frac{89,100\,[\text{kJ/kmol}]}{RT} \tag{6}$$

On the other hand (neglecting the non-ideality of the mixture),

$$\ln K_{x,1} = \frac{\Delta^r S}{R} - \frac{\Delta^r H}{RT} \tag{7}$$

Comparing Eqs. (6) and (7), the reaction enthalpy is $\Delta^r H = 89,100$ kJ/kmol, value which corresponds to a quite endothermal reaction. This apparent endothermal nature of the MH–MeOH etherification contradicts the well-known exothermicity of other alkene–alcohol etherification processes.

For example, the experimentally determined equilibrium constants for etherification of 2,4,4-trimethyl-1-pentene and 2,4,4-trimethyl-2-pentene with methanol are given by Eqs. (8) and (9) (Karinen and Krause, 2001). The heat of reaction are $\Delta^r H = -19,280$ kJ/kmol, respectively $\Delta^r H = -22,786$ kJ/kmol, therefore etherification of both octene isomers is exothermal.

$$K_{244TMP-1} = \exp\left(-8.796 + \frac{2319.03}{T}\right) \tag{8}$$

$$K_{x,244TMP-2} = \exp\left(-8.74 + \frac{2740.7}{T}\right) \tag{9}$$

The reactions between 2-methyl-1-butene or 2-methyl-2-butene leading to *tert*-amyl-methyl ether (TAME) are also exothermal (Kiviranta-Pääkkönen et al., 1999), according to Eqs. (10) and (11).

$$K_{2M1B} = \exp\left(-9.48 + \frac{4382.3}{T}\right) \text{ and } \Delta^r H_{2M1B} = -36,434\ \text{kJ/mol} \tag{10}$$

$$K_{2M2B} = \exp\left(-9.17 + \frac{3520.3}{T}\right) \text{ and } \Delta^r H_{2M2B} = -29,267\ \text{kJ/mol} \tag{11}$$

Studying the etherification of 2-ethyl-1-hexene with methanol, Karinen et al. (2000) found that the equilibrium conversions of 2-ethyl-1-hexene to the ether were 18%, 23% and 27% at the temperatures of 90 °C, 80 °C and 70 °C, respectively. This decrease of equilibrium conversion with temperature is another experimental confirmation of the exothermicity of alkene–alcohol etherification reactions.

We emphasis that experimental data obtained far from equilibrium (initial reaction rates) are usually used to find the forward reaction rate constant ($k_{1,F}$). In contrast, the reverse reaction rate constant $k_{1R}$ is calculated as $k_{1R} = k_{1F}/K_{x1}$, where the equilibrium rate constant $K_{x1}$ should be determined from experiments which proceed close to equilibrium. In this respect, the following statement from the article describing the MH–MeOH etherification (Karinen and Krause, 1999) indicates that there is not enough experimental data from which the equilibrium constant can be precisely determined: "*Since the etherification reaction is very slow it takes a long time to reach thermodynamic equilibrium state. Thus during the experiments the emphasis was laid on the initial rates*".

To elucidate the contradiction between the exothermicity of the etherification reaction found experimentally and the predictions of the kinetic model described by Eqs. (2)–(6), we used the Aspen Plus RGIBBS reactor model to evaluate the equilibrium composition of the MH + MeOH = MMH reaction mixture at different temperature. The RGIBBS model calculates the chemical and phase equilibrium by minimizing the Gibbs free energy of the reacting mixture. For MeOH and MH, all pure component properties (including the ideal gas Gibbs energies of formation, $\Delta G_{f,0}$) are available in Aspen Plus data pure components database. For MMH, $\Delta G_{f,0}$ was estimated by the Joback group contribution method. Group contribution methods were also used for other MMH properties. From the composition of the equilibrium mixture, the equilibrium constant $K_{x,1}$ can be calculated. $K_{x,1}$ values obtained at different temperature were then used to regress the temperature-dependent equilibrium constant parameters. The result, Eq. (12), corresponds to an exothermal reaction:

$$\ln K_{x,1} = -13.659 + \frac{5270.2}{T} \text{ and } \Delta^r H_1 = -43,816\ \text{kJ/mol} \tag{12}$$

Fig. 2 presents the dependence on temperature of the methanol equilibrium conversion, calculated with Eq. (6) — dashed lines, and Eq. (12) — continuous lines, for different values of the initial MH:MeOH ratio, M. First, it is important to note that from a selectivity point of view (for reasons that will be explained later), it is advantageous to operate the reactor at an excess of MH (thus $M > 1$) and high MeOH conversion. In the process described in Luyben (2010), the reactor inlet reactants ratio is $M \approx 2.6$, the reactor is operated at 400 K (123 °C, the maximum value considered to be allowed to avoid catalyst deactivation), and the MeOH conversion is $X_{MeOH} \approx 0.935$.

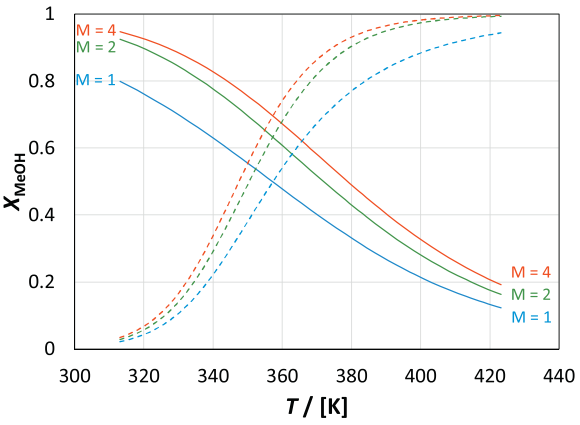


**Fig. 2 – Methanol equilibrium conversion versus temperature in the MH + MeOH = MMH reaction, for different values of the initial MH : MeOH ratio M. Dashed lines: equilibrium constant calculated with Eq. (6). Continuous lines: equilibrium constant calculated by Eq. (12).**

This is easily achievable if the chemical equilibrium is truly described by Eq. (6). For this large value of MeOH conversion, the recycle contains mainly MH and small amounts of MeOH, therefore a relatively small recycle is needed to achieve the required MH:MeOH excess ratio at reactor inlet. Note that the reaction temperature is even higher, for example 423 K in the side reactor–column configuration (Hussain et al., 2019).

On the other hand, if the chemical equilibrium is described be Eq. (12), the methanol conversion achievable at 400 K does not exceed 0.3, even if the MH excess is increased to $M = 4$. Thus, to obtain a large MeOH conversion, say $X_{MeOH} > 0.9$, the reactor should be operated at low temperature, around 320 K. This will result in a slow reaction, requiring extremely large amounts of catalyst. If the reaction temperature is increased, say to 360 K, the reaction is faster but the achievable MeOH conversion is much lower, around 0.7. In this case, the recycle will be larger, with negative consequences on the economics of the process.

## 4. Reaction kinetics

For reversible reaction, the reaction rate constants are usually determined by the following procedure, which minimizes the effect of experimental errors. First, the constant of the forward reaction rate, $k_F$ is found from low-conversion data (initial reaction rate in a batch reactor or reaction rate in a differential reactor). The dependence of the rate constant versus temperature allows determining the activation energy of the forward reaction. Then, the equilibrium constant $K_{eq}$ and its dependence versus temperature is found from experiments in which chemical equilibrium is reached (calculation from thermodynamic principles is also an option). Finally, the reverse reaction rate constant is given by $k_R = k_F/K_{eq.}$ In a different approach, one can first find $K_{eq}$ from equilibrium experiments or from thermodynamic data, and then use time-dependent batch data to regress $k_F$. This approach, in which the forward reaction and equilibrium constants are determined from different experiments was widely applied (see Rahaman et al., 2015; Komon et al., 2013; Ostaniewicz-Cydzik et al., 2014; Buluklu et al., 2014; Leyva et al., 2013; Sert et al., 2013, to name just a few).

Griffin et al. (2009) affirm that kinetic parameters were generated by fitting the kinetic data from Kiviranta-Pääkkönen et al. (1998), Karinen et al. (2001) and Karinen and Krause (1999). The subjects of the first two papers are etherification of isoamylenes, and of 2-methyl-1-butene and 2,4,4-trimethyl-1-pentene. The only experimental data that could be used to find the kinetic parameters of MH–MeOH etherification is presented in Karinen and Krause (1999), which is reproduced here (Fig. 3, left). This figure could be used to find the kinetic parameters (more precisely, the constant of the forward reaction, at different temperatures) of the MH–MeOH etherification, provided some additional information is available: the initial composition of the reaction mixture and the catalyst concentration. The experiments were described as being performed in an 80 $cm^3$ batch reactor, using 1–1.5 g of catalyst. The reaction mixture contained MH and MeOH in a molar ratio between 0.5–2, which was diluted with iso-octane (molar fraction 0.7). As the initial reaction conditions are not exactly known, it is not possible to get a precise value of the reaction rate constant. However, the value of the pre-exponential factor given by Griffin et al. (2009) and used in the previous MMH design studies is reasonable. In fact, at a given temperature, the parameters which determine the performance of a continuous catalytic reactor in which a reversible reaction takes place are the combination of reaction rate constant, mass of catalyst and feed rate, $k_{1F} \times m_{cat}/F$, and the equilibrium constant $K_{eq}$. In practice, when a certain value of conversion is required, the uncertainties in $k_{1F}$ can be compensated by changing the feed rate $F$.

Karinen and Krause (1999) clearly state that the activation energy determined from initial reaction rate (thus concerning the forward reaction) is 90 kJ/mol for MMH formation, value that was used in the previous studies on MMH processes, and which is in line with the activation energy of other etherification processes (e.g. 60–65 kJ/mol for 2,4,4 TMP, Karinen and Krause, 1999).

Fig. 3 (right) presents the calculated alkene conversion in a batch reactor operated at several temperatures, where the initial charge consists of MH, MeOH and iso-octane (0.0533 mol, 0.106 mol, 0.373 mol) and 1 g of catalyst. These conditions are consistent with experiments reported by Karinen and Krause (1999), namely reaction volume 80 $cm^3$, reactants ratio MeOH:MH = 2, iso-octane mole fraction 0.7. The etherification rate was rate was calculated by:

$$r_1 = k_{1F} x_{MeOH} x_{MH} \left(1 - \frac{1}{K_{x,1}} \frac{x_{MMH}}{x_{MeOH} x_{MH}}\right) \quad (13)$$

where $k_{1F}$ and $K_{x,1}$ are given by Eqs. (3) and (12), respectively.

Although not perfect, at 80 °C the agreement with experimental data is reasonable. Therefore, this kinetics will be used in our study.

Several secondary reactions take place during MH–MeOH etherification on Amberlyst 35 catalyst (Karinen and Krause, 1999). First, there is the equilibrium isomerization of 2-methyl-1-heptene to 2-methyl-2-heptene. The later isomer reacts with methanol to give the MMH product. Although the equilibrium is not instantaneous and the isomers have different reactivities, in the previous studies this reaction was neglected and only 2-methyl-1-heptene was considered. This assumption seems reasonable, at least for the purpose of an initial design. Therefore, lumping the two isomers into one component will also be employed in our study.

Other secondary reactions are due to dehydration of methanol, leading to dimethyl ether and water, which also takes place in the presence of the acid catalyst. The water

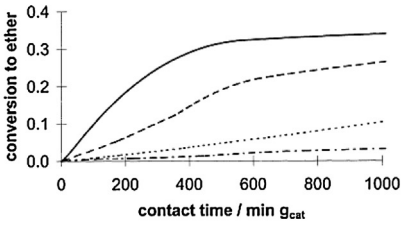


Fig. 2. Conversion to ether in 2-methyl-1-heptene experiments at different temperatures as a function of contact time. 50°C (----), 60°C (----), 70°C (——), 80°C (——).

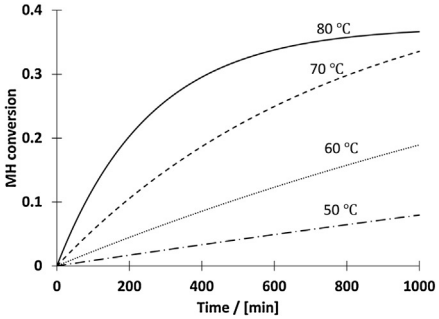


**Fig. 3 – Left: figure with experimental data reported in literature (Karinen and Krause, 1999); Right: calculated MH conversion, initial ratio MeOH:MH = 2, inert mole fraction 0.7, catalyst concentration 0.0125 g/cm$^3$, reaction rate given by Eq. (13).**

resulted from this reaction reacts irreversible with the alkene, leading to a tertiary alcohol. This reaction is fast.

$$\underset{(MeOH)}{2CH_3OH} \rightleftarrows \underset{(DME)}{CH_3OCH_3} + \underset{(W)}{H_2O} \tag{14}$$

$$\underset{(W)}{H_2O} + \underset{(MH)}{C_8H_{16}} \rightarrow \underset{(MHOH)}{C_8H_{17}OH} \tag{15}$$

The overall reaction is:

$$\underset{(MeOH)}{2CH_3OH} + \underset{(MH)}{C_8H_{16}} \rightarrow \underset{(DME)}{CH_3OCH_3} + \underset{(MHOH)}{C_8H_{18}O} \tag{16}$$

The rate of Reaction (16) is equal to the rate of the slow (limiting) step, therefore:

$$r_2 = k_2(x_{MeOH})^2 \tag{17}$$

where

$$k_2 / \left[\text{kmols}^{-1}\ \text{kg}_{\text{cat}}^{-1}\right] = 1.3 \times 10^9 \cdot \exp\left(-\frac{105,900\ [\text{kJ/kmol}]}{RT}\right) \tag{18}$$

There is little experimental information to check the correctness of Eq. (18). Regarding the etherification of isoamylenes with methanol, Kiviranta-Pääkkönen et al. (1998) found $k_{(343K)} = 4.95 \times 10^{-5}$ mol/kg/s and $E_a = 102,600$ kJ/kmol as kinetic parameters of MeOH dehydration to DME (a LHHW mechanism was assumed). The values given by Griffin et al. (2009), namely $14.1 \times 10^{-5}$ mol/kg/s and 105,900 kJ/kmol, are the same order of magnitude. Hence, we accept Eqs. (17) and (18) to represent the kinetics of the secondary Reaction (16).

## 5. Reactor design

The reaction system can be well described by the parallel–consecutive Reactions (1) (which gives the MMH product) and (16) (in which MH is transformed into the by-products DME and MHOH). The common reactant involved in both reactions is MeOH. To favor the main reaction and achieve high selectivity, MeOH concentration must be kept low. The activation energies of the main and secondary reaction (90,000 kJ/kmol vs. 105,900 kJ/kmol), indicate that high temperature slightly favors the secondary reaction, thus decreasing the selectivity.

The flowsheet proposed by Luyben (2010) uses a Continuous Stirred Tank Reactor (CSTR). The reactor contains about 10,000 kg of catalyst, has a volume of 12 m$^3$ and is operated at 400 K, which is considered to be the maximum temperature allowed by the catalyst. The reaction temperature is maintained by 12,175 kg/h of cooling water, at 350 K. The heat transfer area is 25.1 m$^3$ and the heat transfer coefficient is 0.57 kW/m$^2$/K — quite a large value which would require vigorous mixing of the reactor contents. We remark that cooling the reactor indicates an exothermal reaction, in agreement with Eq. (12) and contradicting Eq. (6). We also note that the perfect mixing assumption means that the species concentrations at any point inside the reactor and in the outlet stream are the same – in particular the MeOH concentration is very low throughout the entire reactor. In other words, in a CSTR, if one can achieve high methanol conversion (for example by feeding the reactor with an excess of MH and by using a large amount of catalyst), then the goal of high selectivity is easily accomplished because MeOH concentration is low. However, perfectly mixing such a large amount of solid catalyst seems a very difficult task. Therefore, a fixed-bed catalytic reactor is more appropriate. Firstly, we note that in a plug flow reactor the reactants concentration gradually changes along the reactor length, thus the condition of low MeOH concentration cannot be fulfilled everywhere in the reactor. Secondly, in the case of a fixed bed reactor, the heat transfer is limited. As the reaction takes place in liquid phase, the velocity of the reaction mixture through the catalyst bed cannot be too high, otherwise the pressure drop will be excessively large. On the other hand, at low velocities the partial heat transfer coefficient from the reaction mixture to the wall is small. One can increase the heat transfer area by using a multitubular reactor, with small diameter of the tubes, but this also increases the pressure drop. Therefore, adiabatic operation is the best way to operate the reactor. However, the temperature increase leads to a lower equilibrium conversion, putting thus a limit on the achievable conversion. One solution, that will be considered in our study, is to use a multi-bed reactor with intermediate cooling. The alternative of a cooled multi-tubular reactor proved to be more expensive.

## 6. Results and discussion

This section presents the production process of 54.87 ktpy MMH of 99.2%wt. purity. This corresponds to 50 kmol/h fresh MeOH (limiting reactant) rate, which is the same as in MMH processes presented in literature and allows for a fair direct

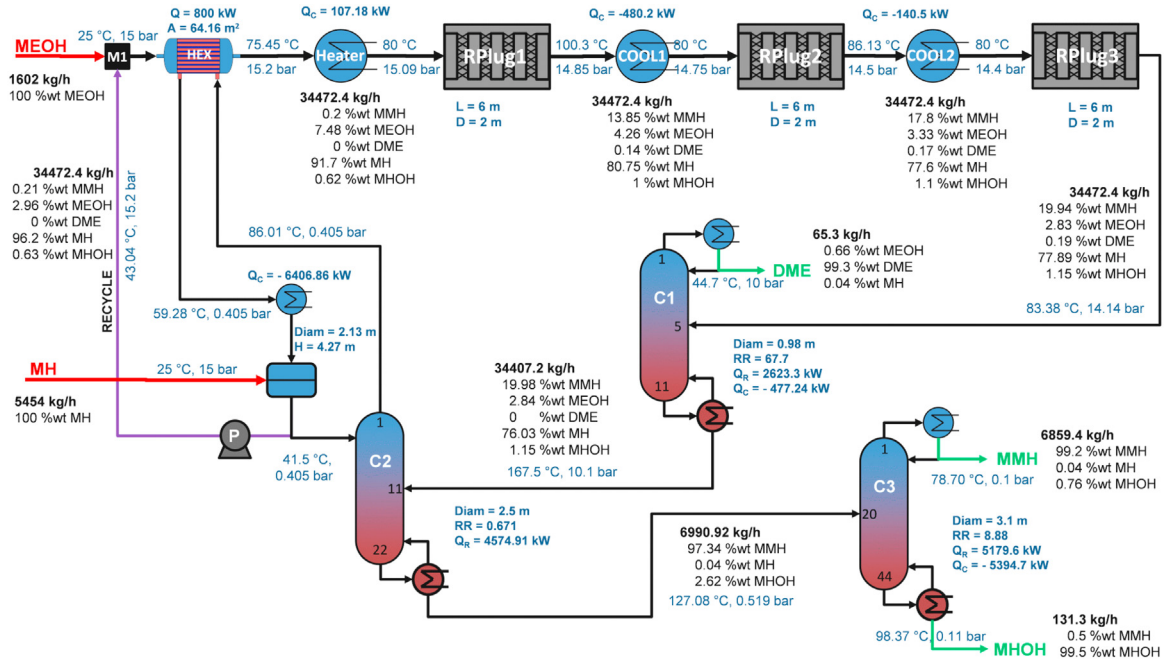


**Fig. 4 – Flowsheet of the MMH process.**

comparison. The mass balance and key design parameters are shown in Fig. 4.

### 6.1. *Process design*

Fig. 4 presents the flowsheet of the MMH process, the mass balance and the key design parameters. The fresh MH is fed to the reflux drum of the column C2 which recovers the reactants. The distillate of C2 (containing mainly MH and MeOH) is mixed with fresh MeOH, brought to 80 °C, and fed to the first catalytic bed. After mixing, the molar reactants ratio is MH:MeOH = 3.5. The first reactor has 2 m diameter, 6 m lengths and contains 18,840 kg of catalyst. The reactor is operated adiabatically. At the exit of the reactor, MeOH conversion is 0.43 and the temperature increases to 100.3 °C. As the reaction slows down due to approaching the equilibrium, the mixture is cooled down to 80 °C before entering the second reactor (diameter 2 m, length 6 m, 18,840 kg catalyst, outlet temperature 86.13 °C). Here, MeOH conversion increases to 0.55. The mixture is again cooled to 80 °C and passed through the third catalytic bed (18,840 kg catalyst). MeOH conversion increases to 0.62, and the temperature reaches 83.38 °C. The selectivity achieved is 0.95 kmol MMH / kmol MeOH. As an alternative, a multi-tubular reactor could be used. The same MeOH conversion and a slightly lower selectivity (0.93 kmol MMH/kmol MeOH) could be achieved using the same amount of catalyst in a multi-tubular reactor (3200 tubes of 5 cm diameter), cooled with 36,000 kg/h water (78 °C inlet temperature, 91.36 °C outlet temperature, heat transfer coefficient 0.1 kW/m$^2$/K).

Fig. 5 shows, in a conversion–temperature diagram, the course of the reaction in the three-bed reactor system with inter-stage cooling (continuous line) and in the cooled multi-tubular reactor (dashed line). The equilibrium MeOH conversion (calculated considering the reaction MeOH + MH = MMH) is also presented.

The effluent of the reaction section is fed to the first distillation column (C1) which separates the DME by-product. The column has 11 theoretical stages (sieve trays) and is operated at 10 bar. DME is obtained as distillate byproduct with 0.993%wt. purity. The column completely recovers the MeOH reactant (less than 0.1% of the fresh MeOH is lost in C1 distillate).

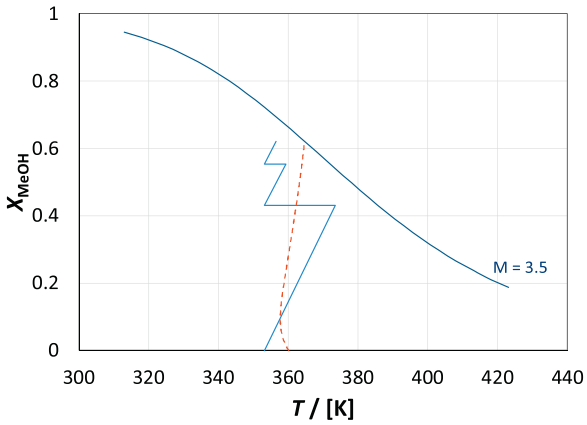


**Fig. 5 – MeOH conversion vs. temperature diagram, showing the reaction course along the three adiabatic catalytic reactors with inter-stage cooling (continuous line) and one multi-tubular cooled reactor (dashed line), and the equilibrium conversion.**

Column (C2) separates the reactants MeOH and MH as distillate, which is recycled, while the bottoms contain a MMH – MHOH mixture. The column has 21 theoretical stages (structured packing, height 17.4 m, diameter 2.5 m) and is operated at 0.405 bar to allow use of cooling water in condenser and low-pressure steam in reboiler. Note that before condensing, the vapor distillate is used to pre-heat the reactor feed. Moreover, the fresh MH is fed in the condenser drum of this column. The last column (C3) has 44 theoretical stages (structured packing, 3.1 m diameter, 16.4 m height) and is operated under vacuum (0.1 bar) to achieve the difficult MMH–MHOH separation. The MMH product is obtained as distillate at 0.992%wt purity.

Fig. 6 shows the temperature and liquid mass fraction profiles in the distillation columns.

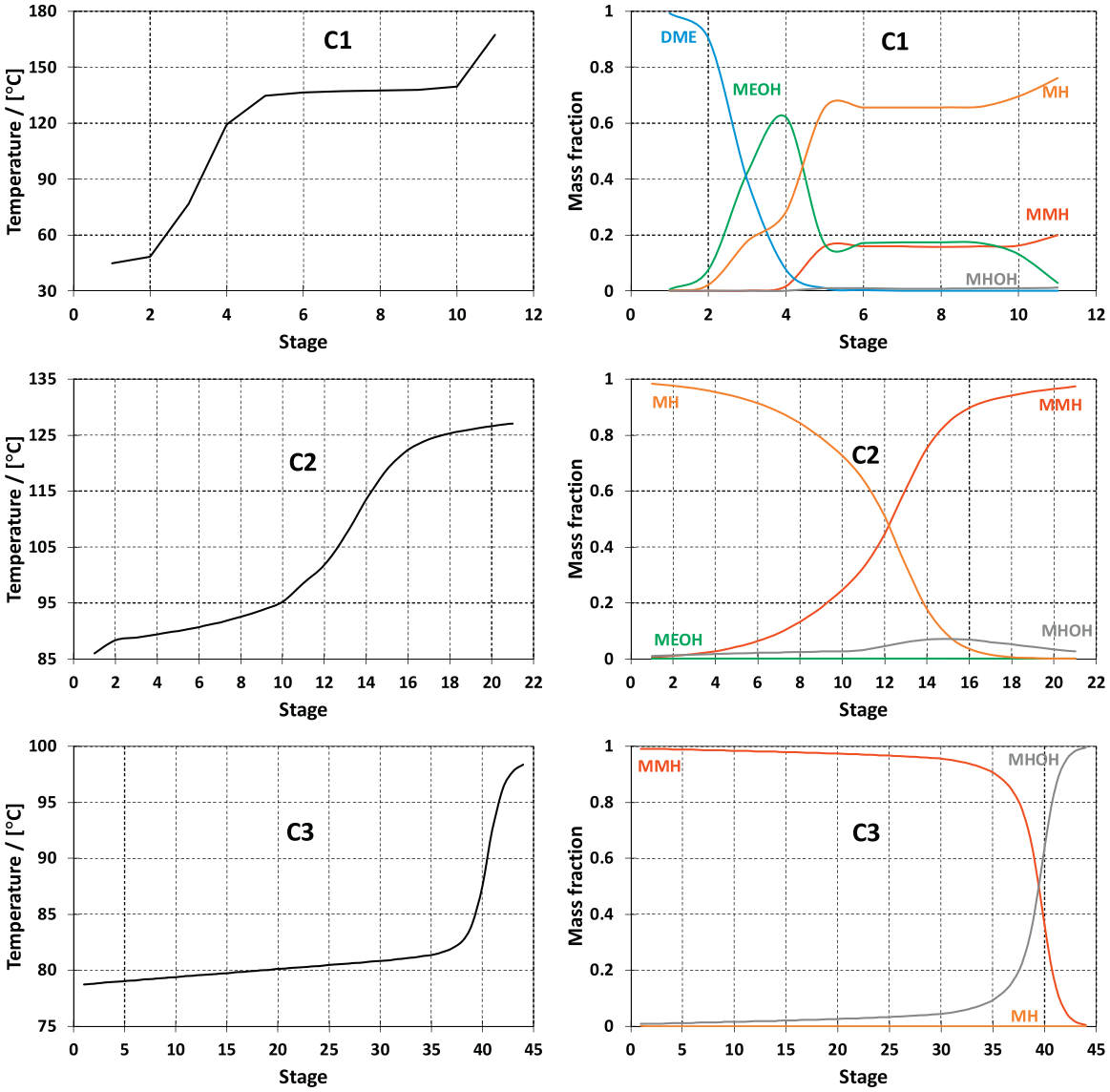


**Fig. 6 – Temperature and composition profiles of the distillation columns.**

Overall, the process produces 47.59 kmol/h MMH, which corresponds to a yield of 0.95 kmol MMH/kmol MeOH, or 0.98 kmol MMH/kmol MH.

For a fair comparison with previous studies, the process presented here assumes pure feed streams. If there are some light impurities (for example, formaldehyde in fresh MeOH), they will leave the process with the DME stream. Such impurities are expected in very small amounts, as MeOH is usually obtained at high purity.

Impurities are most likely to be found in the MH feed. Here, one can distinguish:

- Heavy impurities, which will leave the process with the MHOH by-product.
- Intermediate, reacting impurities (for example, isomers of 2-methyl 2-heptene), which will be consumed in the reaction, leading to by-products with properties similar to MMH. These by-products will likely impurify the MMH product.
- Inert, intermediate impurities (such as octane isomers), which are troublesome. With the current process structure, such impurities will be recycled and will accumulate in the process. To cope with such impurities, the process must be modified, for example by purifying the feed stream, or by including additional separation units to remove the inert from the recycle stream. There is also the option of a bleed stream. We emphasize that is not a control, but a design problem.

### 6.2. *Economic evaluation*

The capital cost was evaluated according to Dimian (2003).

$$TAC = OPEX + \frac{CAPEX}{payback\ period} \tag{19}$$

The heating and cooling costs considered are: LP steam (6 bar, 160 °C, $7.78/GJ), MP steam (11 bar, 184 °C, $8.22/GJ), and cooling water (1 bar, 25 °C $0.72/GJ). The total investment costs (CAPEX) include the reactors, distillation columns, heaters and coolers.

The cost of the equipment is estimated by standard cost correlations:

$$C_{HEX}\,(US\$) = (M\&S/280) \cdot \left(474.7 \cdot A^{0.65}\right)(2.29 + F_m\,(F_d + F_p)) \tag{20}$$

**Table 1 – Economic evaluation of the process.**

| Item description (unit) | C1 | C2 | C3 | Reactors | Heater | Coolers | HEX | Total |
|---|---|---|---|---|---|---|---|---|
| Shell/[$10^3$ US$] | 97.0 | 482.4 | 968.3 | 159.4 | 31.2 | 191.8 | 50.4 | 1980.6 |
| Trays/[$10^3$ US$] | 6.1 | – | – | – | – | – | – | 6.1 |
| Packing/[$10^3$ US$] | – | 64.8 | 199.2 | – | – | – | – | – |
| Reboiler / [$10^3$ US$] | 697.3 | 638.5 | 460.4 | – | – | – | – | 1796.2 |
| Condenser/[$10^3$ US$] | 215.8 | 1277.1 | 468.7 | – | – | – | – | 1961.6 |
| Reflux drum/[$10^3$ US$] | 25.8 | 128.7 | 114.4 | – | – | – | – | – |
| Catalyst/[$10^3$ US$] | – | – | – | 565.0 | – | – | – | 565.0 |
| CAPEX/[$10^3$ US$/ year] | 347.3 | 863.8 | 737.0 | 241.5 | 10.4 | 63.9 | 16.8 | 2103.1 |
| Heating/[$10^3$ US$/year] | 621.0 | 1025.1 | 1160.6 | – | 24.0 | – | – | 2830.7 |
| Cooling/[$10^3$ US$/year] | 9.9 | 132.9 | 111.9 | – | – | 12.9 | – | 267.5 |
| OPEX/[$10^3$ US$/year] | 630.9 | 1157.9 | 1272.4 | 0.0 | 24.0 | 12.9 | 0.0 | 3098.2 |
| TAC/[$10^3$ US$/year] | 969.6 | 1978.9 | 1971.3 | 241.5 | 34.4 | 76.8 | 16.8 | 5289.3 |

where M&S is the Marshall & Swift equipment cost index (M&S = 1638.2 in 2018), A is the area ($m^2$), $F_m = 1$ (carbon steel), $F_d = 0.8$ (fixed-tube), $F_p = 0$ (less than 20 bar). A heat transfer coefficient $U = 850$ kcal/$m^2$/h/K was assumed to calculate the heat transfer area. For the reboilers, the design factor was taken as $F_d = 1.35$.

The diameters of the distillation columns (D) were obtained by the "Internals" utility from Aspen Plus, while the height was evaluated as $H = 0.6 \cdot (NT\text{-}1) + 2$ (m) for the tray column C1 and as HETP·NT + 2 (m) for the packed columns C2 and C3. Afterwards, the cost of the columns shells was calculated as:

$$C_{shell}\,(US\$) = (M\&S/280) \cdot \left(957.9 \cdot D^{1.066} \cdot H^{0.82}\right) \cdot (2.18 + F_c) \quad (21)$$

where $F_c = F_m \cdot F_p$, $F_m = 1$ (carbon steel) and

$$F_p = 1 + 0.0074 \cdot (P - 3.48) + 0.00023 \cdot (P - 3.48)^2$$

The cost of the trays was given by:

$$C_{trays}\,(US\$) = N_T \cdot (M\&S/280) \cdot 97.2 \cdot D^{1.55} \cdot (F_t + F_m) \quad (22)$$

with $F_t = 0$ (sieve trays) and $F_m = 1$ (carbon steel).

The cost of the packing was given by:

$$C_{packing}\left(US\$\right) = \pi \cdot D^2/4 \cdot HETP \cdot NT \cdot packing\,cost \quad (23)$$

According to the literature (Kiss, 2013), a typical price for random packing stainless steel type is about 1500 $/$m^3$.

The cost of the catalyst was given by:

$$C_{reactors}\left(US\$\right) = \pi \cdot D^2/4 \cdot L_{reactor} \cdot \rho_{cat} \cdot cost_{cat} \quad (24)$$

where $L_{reactor}$ is the length of reactor, D is the diameter of reactor, $\rho_{cat}$ is the density of the catalyst and $cost_{cat}$ is the cost of the catalyst (10 $/kg).

The cost of the equipment (CAPEX) and operating (OPEX) are given in Table 1. A payback period of 3 years and 8000 h/year operating time were assumed. The total annual cost is evaluated at $5289 \times 10^3$ US$/year. This is considerably larger compared to original the design (Luyben, 2010, $1343.6 \times 10^3$ US$/year, at 0.98 kmol MMH/kmol MeoH yield), optimized and dividing-wall processes (Hussain et al., 2021), $920 \times 10^3$ US$/year and $814 \times 10^3$ US$/year, at 0.982 kmol MMH/kmol MeOH yield), reactive distillation process (Hussain et al., 2018, $1198 \times 10^3$ US$/year at 0.98 kmol MMH/kmol MeOH yield) or the heat integrated, side reactor–column configuration (Hussain et al., 2018, $1010 \times 10^3$ US$/year at 0.986 kmol MMH/kmol MeOH yield). The specific TAC is 96.4 $/tonne MHOH. We also note that the raw materials costs can be evaluated at $5126 \times 10^3$ US$/year (methanol, 400 $/tonne, alibaba.com) and $43{,}632 \times 10^3$ US$/year (2-methyl-1-heptene, 1000 $/tonne, guidechem.com), for a total of 888 $/tonne MMH, much larger than the investment and operating costs. Thus, the profitability of the process will largely depend on the selling price of the MMH product.

As previously mentioned, the use of a multi-tubular cooled reactor is a feasible option. However, the cost of the cooled multi-tubular reactor ($800.8 \times 10^3$ US$) is much larger compared to the cost of 3 adiabatic reactors and 2 intermediate coolers ($351.2 \times 10^3$ US$).

The effect of increasing the MH excess at the reactor inlet, from a ratio of MeOH/MH = 3.5–4.5 (mole based), was also investigated. The overall yield increases, from 0.98 to 0.985 kmol MMH / kmol MH. However, the energy requirements of columns C1 and C2 almost double, from 3.14 + 4.66 = 7.8 MW to 5.89 + 8.34 = 14.23 MW. In the absence of a reliable value of the MMH price, it is difficult to assess whether the slight increase in the process yield justifies the much higher energy requirements.

### 6.3. *Dynamics and process control*

The plantwide control structure is given in Fig. 7, while the controller tuning parameters are listed in Table 2. The plantwide control structure, follows from the considerations explained in detail in Dimian et al. (2014). The MMH plant is a two-reactant process, with the reactants being recycled together. In this case, the recommended control strategy is to fix the flow rate of the fresh limiting reactant (MeOH) and to use this flow rate as throughput manipulator. The reactor-inlet flow rate of the stream obtained after mixing the fresh excess reactant (MH) with the recycle is ratioed to the flow of fresh limiting reactant. The fresh excess reactant is added to control the inventory in C2 condenser drum. This strategy reduces the interaction between the reaction and the separation section, as it effectively cuts the recycle loop. The rest of the control structure is standard, including pressure control for distillation columns, level control for all liquid vessels (including reflux drums and sumps), temperature control of the heater and coolers, and temperature control of the distillation (two-point control for columns C-1 and C2, one-point temperature control for columns C2 and C3).

A flow-driven dynamic simulation was built in Aspen Plus Dynamics. In a flow-driven simulation, flow rates are specified. Thus, the flow-control loops shown in Fig. 7 are not explicitly modelled, although they do exist in a real plant. The Aspen Plus Dynamics simulation used instantaneous models (HEATER) for the heat exchangers. Because

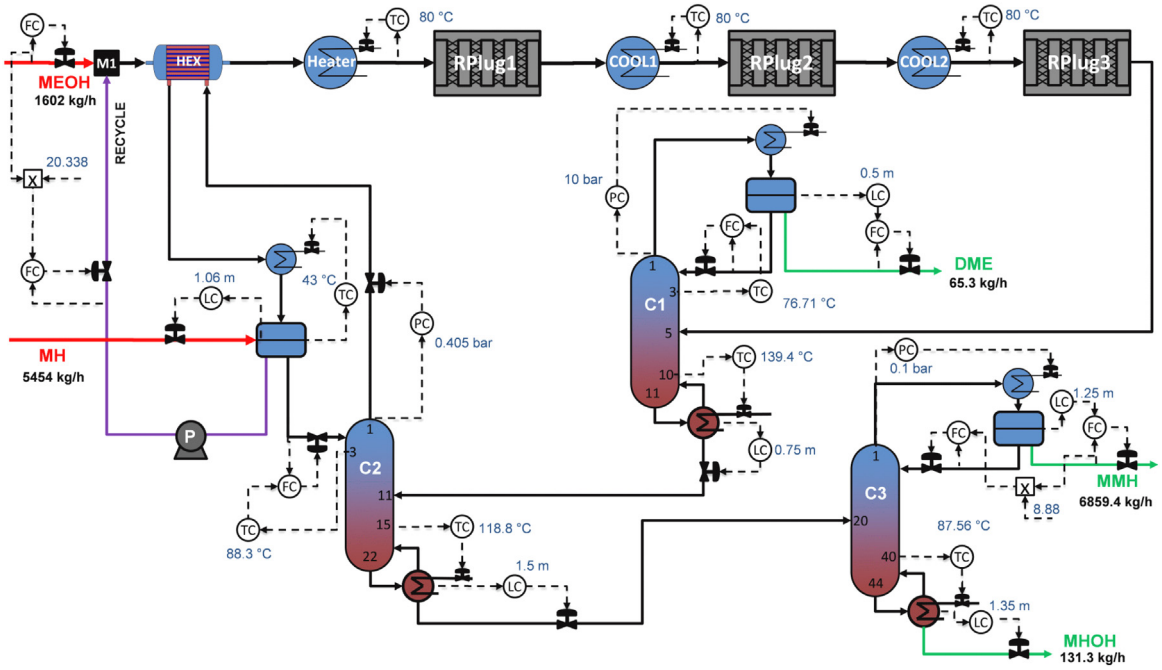


**Fig. 7 – Process control structure of MMH production plant.**

**Table 2 – Controller tuning parameters.**

| Controller | PV, value & range | OP, value & range | Kc, [%OP]/[%PV] | Ti, min |
|---|---|---|---|---|
| FC MEOH | Flow rate = 1602.11 kg/h | | | |
| LC reflux drum C2 | Level = 0.76 m<br>0. . .2.13 m | Flow rate MH = 5454 kg/h<br>0. . .10907.9 kg/h | 1 | 600 |
| RATIO control | Flow rate MHmix = 32,945.6 kg/h | Flow rate MEOH = 1602.11 kg/h | ratio = 20.34 | |
| PC C1 | Column pressure = 10 bar<br>0 . . . 20 bar | Condenser duty = −1.88 GJ/h<br>−5.4. . .0 GJ/h | 20 | 12 |
| LC reflux drum C1 | Level = 0.5 m<br>0. . .1 m | Distillate rate = 65.24 kg/h<br>0. . .130.4 kg/h | 1 | 600 |
| LC sump C1 | Level = 0.75 m<br>0. . .1.5 m | Bottom flow rate = 34482.4 kg/h<br>0. . .68814.4 kg/h | 1 | 600 |
| TC stage 3 C1 | Temperature = 76.71 °C<br>60 . . . 120 °C | Reflux Rate = 4858.05 kg/h<br>0. . .30,000 kg/h | 0.07 | 6.6 |
| TC stage 10 C1 | Temperature = 139.4 °C<br>130 . . .150 °C | Reboiler duty = 9.63 GJ/h<br>0. . .18.88 GJ/h | 0.46 | 6.6 |
| PC C2 | Column pressure = 0.405 bar<br>0.38 . . . 0.42 bar | Top vapor flow = 577.05 kmol/h<br>0 . . .1151 kmol/h | 1 | 12 |
| LC reflux drum C2 | Level = 0.76 m<br>0. . .2.13 m | Flow rate MH = 5454 kg/h<br>0. . .10907.9 kg/h | 1 | 600 |
| LC sump C2 | Level = 1.5 m<br>0. . .3 m | Bottom flow rate = 6990.8 kg/h<br>0. . .28,000 kg/h | 1 | 600 |
| TC condenser C2 | Temperature = 41.5 °C<br>30 . . .50 °C | Condenser duty = −23.12 GJ/h<br>−100. . .0 GJ/h | 1 | 20 |
| TC stage 15 C2 | Temperature = 118.8 °C<br>100 . . .140 °C | Reboiler duty = 16.5 GJ/h<br>0. . .100 GJ/h | 0.04 | 13.2 |
| TC stage 2 C2 | Temperature = 88.3 °C<br>70 . . . 110 °C | Reflux Rate = 32490.26 kg/h<br>0. . .128,000 kg/h | 5.54 | 10.56 |
| PC C3 | Column pressure = 0.1 bar<br>0.095 . . . 0.105 bar | Condenser duty = −19.42 GJ/h<br>−38.84. . .0 GJ/h | 1 | 12 |
| LC reflux drum C3 | Level = 1.25 m<br>0. . .2.5 m | Distillate flow rate = 6859.37 kg/h<br>0. . .13718.9 kg/h | 1 | 600 |
| LC sump C3 | Level = 1.35 m<br>0. . .2.7 m | Bottom flow rate = 131.49 kg/h<br>0. . .362.8 kg/h | 1 | 600 |
| TC stage 40 C3 | Temperature = 88.5 °C<br>80 . . . 100 °C | Reboiler duty = 18.64 GJ/h<br>0. . .37.29 GJ/h | 0.21 | 9.24 |

in practice controlling the outlet temperature of a heat exchanger is an easy task, good temperature control was assumed; therefore, the default model settings were changed from specified duty (calculated outlet temperature) to specified temperature (calculated duty). Thus, implementation of heat-exchangers temperature control loops was not necessary.

All controllers are proportional-integral (PI) type. For the distillation temperature control loops a measurement dead time of 1 min was assumed. To tune the distillation temper-

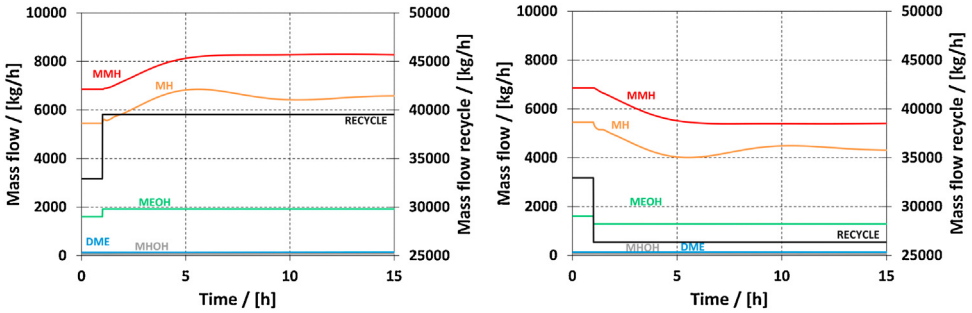


**Fig. 8 – Mass flow of the main streams in MMH production plant during 20% production rate increase (left) or decrease (right).**

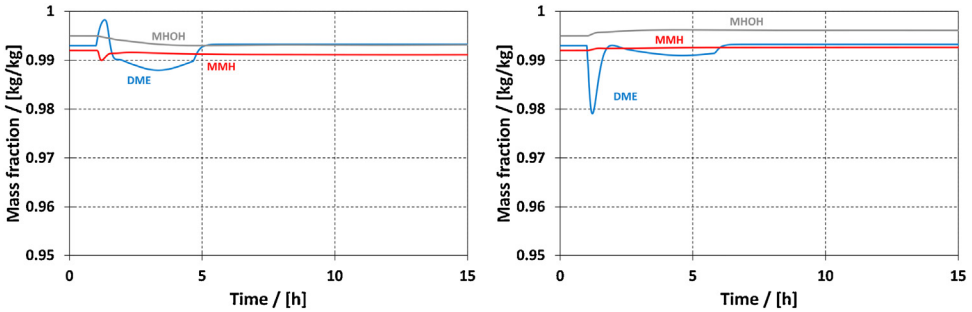


**Fig. 9 – Mass fraction in the product streams of the MMH plant during 20% production rate increase (left) or decrease (right).**

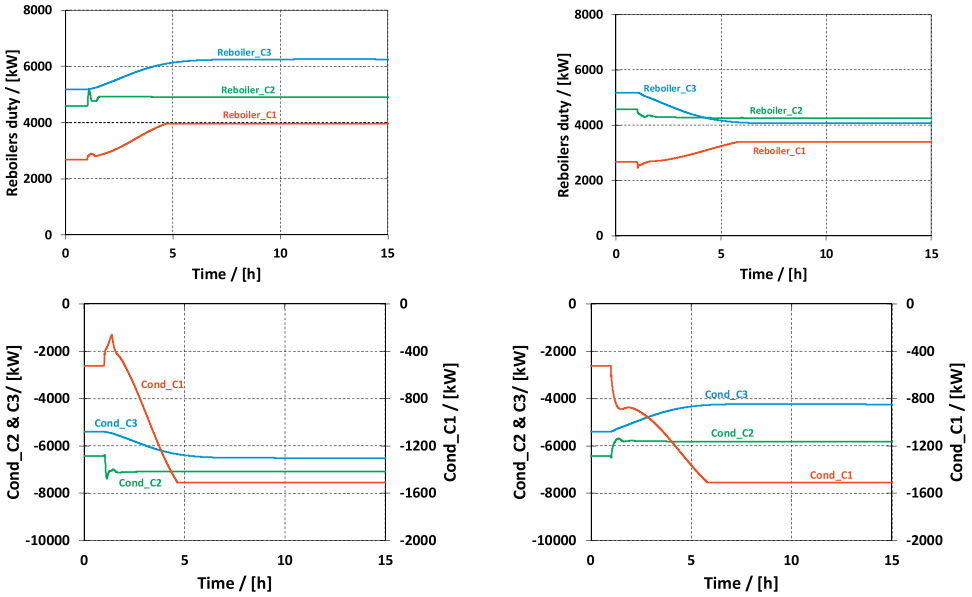


**Fig. 10 – Energy requirement in distillation columns during 20% production rate increase (left) or decrease (right).**

ature controllers, the stability limit was found by the auto tune variation (ATV) method, and the parameters were set according to the Tyreus-Luyben rules (Luyben, 2011). For other controllers, the process variable (PV) and controller output (OP) ranges were set based on engineering heuristics. The controller gain was set to $Kc = 1$[%OP_range]/[%PV_range] and the integral time $Ti$ to the estimated value of the process time constant. For the level controllers, a large value of the integral time was used.

The performance of the control structure is tested for variation of ±20% of the production rate. After 2 h of steady-state operation, the methanol feed rate is changed by ±20%. The ratio controller ensures the necessary excess of MH by increasing or reducing the flow of liquid (MH + MeOH) removed from C2 condenser drum, while the level controllers changes the flow rate of fresh MH to control the inventory. Fig. 8 shows the mass flow of the main streams of the process (+20% production rate changes — left plot; −20% production rate changes — right plot).

The flow rate of each stream follows the positive/negative changes introduced in the process. The quality of the products (MMH, DME, and MHOH) remains almost unchanged, reaching a new steady state in a short time after the production rate was changed (Fig. 9).

Fig. 10 shows the change in distillation energy requirements while changing the production rate. Increasing the production rate by 20%, the duties in columns C1, C2 and C3 increase by 47%, 7%, 20%, (heating) and 188%, 10% and 20%,

(cooling) respectively. The rather high sensitivity of column C1 should be remarked. Interestingly, when the production rate decreases by 20%, the duties of column C1 increase by 27% (heating) and 188% (cooling). The behavior of column C2 and C3 is more typical, as the duties decrease by 7% and 20% (heating) and 9.5% and 20% (cooling).

## 7. Conclusions

This article illustrates the importance of carefully checking the design basis data. Considering the etherification of 2-methyl-1-heptene with methanol to produce 2-methoxy-2-methyl heptane, the designs previously reported were analyzed, and the following issues were identified and properly address in this work that critically rethinks the design of the process:

- When the vapor pressure of the by-product 2-methyl-2-heptanol is calculated by the extended Antoine model with parameters estimated by the Riedel model, the predicted volatility is much lower compared to the one calculated by the Wagner 25 equation with NIST-TRC parameters. The later method is more sensible, as it gives a normal boiling point close to the one reported experimentally. Thus, the purification of the MMH product is difficult, requiring high capital and operating expenses.
- The etherification reaction is exothermal, but the previous studies considered a kinetic expression compatible with an endothermal reaction. If this was true, the optimal reaction temperature is the maximum one allowed by the catalyst. In this study, the kinetics was adjusted to correctly represents the rate of an exothermal reaction. As a result, the reaction temperature should be much lower, to avoid the equilibrium limitations. Therefore, much larger amounts of catalysts are needed.
- Perfect mixing and temperature control of reactors employing large amounts of catalyst is very difficult. The practical solution is to use adiabatic fixed bed reactors (with intermediate cooling due to the exothermal nature of the reversible reaction). However, high selectivity is more difficult to be achieved, requiring a larger excess of MH reactant. This has to be separated and recycled, with the drawback of higher operating costs.

The process developed here is more realistic, but as expected it requires a larger investment and it is more energy intensive (2.29 kW h/kg MMH) as compared to previously reported studies which used unreliable kinetics and thermodynamics, underestimating the challenges.

For a plant capacity of 54.87 ktpy 2-methoxy-2-methyl-heptane, the total annualized cost is 5.3 M$/year, or 96.4 $/tonne product. As this value is lower than the raw material costs (888 $/tonne), the profitability of the plant will largely depend on the selling price of the product. Inert impurities in the olefin feed will worsen the economics, as they will require additional separation units. The designed process is stable and able to reject disturbances at ±20% production rate changes.

## Declaration of interests

The authors declare that they have no known competing financial interests or personal relationships that could have appeared to influence the work reported in this paper.

## Declaration of Competing Interest

The authors report no declarations of interest.

## References


Buluklu, A.S., Sert, E., Karakus, S., Atalay, F.S., 2014. Development of kinetic mechanism for the esterification of acrylic acid with hexanol catalyzed by ion-exchange resin. Int. J. Chem. Kinet. 46 (4), 197–205, http://dx.doi.org/10.1002/kin.20841.

Dimian, A.C., 2003. Integrated Design and Simulation of Chemical Processes. Elsevier, Amsterdam.

Dimian, A.C., Bildea, C.S., Kiss, A.A., 2014. Integrated Design and Simulation of Chemical Processes, 2nd edition. Elsevier, Amsterdam.

Griffin, D.K., Mellichamp, D.A., Doherty, M.F., 2009. Effect of competing reversible reactions on optimal operating policies for plants with recycle. Ind. Eng. Chem. Res. 48, 8037–8047.

Hussain, A., Lee, M., 2018. Optimal design of an intensified column with side-reactor configuration for the methoxy-methylheptane process. Chem. Eng. Res. Des. 136, 11–24.

Hussain, A., Minh, L.Q., Qyyum, M.A., Lee, M., 2018. Design of an intensified reactive distillation configuration for 2-methoxy-2-methylheptane. Ind. Eng. Chem. Res. 57, 316–328.

Hussain, A., Chaniago, Y.D., Riaz, A., Lee, M., 2019. Significance of operating pressure on process intensification in a distillation with side-reactor configuration. Sep. Purif. Technol. 213, 533–544.

Hussain, A., Qyyum, M.A., Minh, L.Q., Riaz, A., Haider, J., Naqvi, M., Naqvi, S.R., Lee, M., 2021. Methoxy-methylheptane as a cleaner fuel additive: an energy-and cost-efficient enhancement for separation and purification units. Energy Sci. Eng. 9, 632–1646.

Karinen, R.S., Krause, A.O.I., 1999. Reactivity of some C8-alkenes in etherification with methanol. Appl. Catal. A: Gen. 188, 247–256.

Karinen, R.S., Krause, A.O.I., 2001. Kinetic model for the etherification of 2,4,4-trimethyl-1-pentene and 2,4,4-trimethyl-2-pentene with methanol. Ind. Eng. Chem. Res. 40, 6073–6080.

Karinen, R.S., Krause, A.O.I., Tikkanen, E.Y.O., Pakkanen, T.T., 2000. Catalytic synthesis of a novel tertiary ether, 3-methoxy-3-methyl heptane, from 1-butene. J. Mol. Catal. A: Chem. 152, 253–255.

Karinen, R.S., Linnekoski, J.A., Krause, A.O.I., 2001. Etherification of C5 and C8 alkenes with C1 to C4 alcohols. Catal. Lett. 76, 81–87.

Kiss, A.A., 2013. Advanced Distillation Technologies. Wiley, Chichester.

Kiviranta-Pääkkönen, P.K., Struckmann, L.K., Linnekoski, J.A., Krause, A.O.I., 1998. Dehydration of the alcohol in the etherification of isoamylenes with methanol and ethanol. Ind. Eng. Chem. Res. 37 (18), 1198.

Kiviranta-Pääkkönen, P., Struckmann, L., Krause, A.O.I., 1999. Comparison of the various kinetic models of TAME formation by simulation and parameter estimation. Chem. Eng. Technol. 21 (4), 321–326.

Komon, T., Niewiadomski, P., Oracz, P., Jamróza, M., 2013. Esterification of acrylic acid with 2-ethylhexan-1-ol: thermodynamic and kinetic study. Appl. Catal. A: Gen. 451, 127–136.

Leyva, F., Orjuela, A., Miller, D.J., Gil, I., Vargas, J., Rodríguez, G., 2013. Kinetics of propionic acid and isoamyl alcohol liquid esterification with Amberlyst 70 as catalyst. Ind. Eng. Chem. Res. 52, 18153–18161.

Luyben, W.L., 2010. Design and control of the methoxy-methyl-heptane process. Ind. Eng. Chem. Res. 49, 6164–6175.

Luyben, W.L., 2011. Principles and Case Studies of Simultaneous Design. Wiley, Hoboken.

Ostaniewicz-Cydzik, A.M., Pereira, C.S.M., Molga, E., Rodrigues, A.E., 2014. Reaction kinetics and thermodynamic equilibrium for butyl acrylate synthesis from *n*-butanol and acrylic acid. Ind. Eng. Chem. Res. 53, 6647–6654.

Rahaman, M., Graça, N.S., Pereira, C.S.M., Rodrigues, A.E., 2015. Thermodynamic and kinetic study of the production of oxygenated compounds: synthesis of 1,1-diethoxybutane catalyzed by amberlyst-15. Can. J. Chem. Eng. 93 (11), 1990–1998.

Sert, E., Buluklu, A.D., Karakus, S., Atalay, F.S., 2013. Kinetic study of catalytic esterification of acrylic acid with butanolcatalyzed by different ion exchange resins. Chem. Eng. Process. Process. Intensif. 73, 23–28.